

Effect of 211 inclusions in directionally melt-textured $(Y_{0.5}Sm_{0.25}Nd_{0.25})Ba_2Cu_3O_y$ oxides

So-Jung Kim*

Department of Electrical and Electronic Engineering, Hanzhong University, Donghae, Gangwon 240-713, Korea

Directionally melt-textured high T_c $(Y_{0.5}Sm_{0.25}Nd_{0.25})Ba_2Cu_3O_y$ [(YSN)-123] composite superconductors with and without CeO_2 additive were systematically investigated by the zone melt growth process in air. A sample prepared by this method showed a well-textured microstructure, and $(Y_{0.5}Sm_{0.25}Nd_{0.25})_2BaCuO_5$ [(YSN)211] inclusions were uniformly dispersed in a large grained (YSN)123 matrix. The size of (YSN)211 inclusions in melt-textured (YSN)-123 with the CeO_2 additive were remarkably reduced within the (YSN)123 matrix. Both samples, with and without the CeO_2 additive, showed an onset $T_c \geq 94$ K and a sharp superconducting transition. The magnetization values of (YSN)-123 with the CeO_2 additive, were higher ($M=500$ emu/cm³ in 4 Tesla at 50 K) than those of (YSN)-123 without the CeO_2 additive.

Key words: $(Y_{0.5}Sm_{0.25}Nd_{0.25})Ba_2Cu_3O_y$, composite, zone melt growth, $(Y_{0.5}Sm_{0.25}Nd_{0.25})_2BaCuO_5$, inclusion, magnetization.

Introduction

Directionally melt-textured high T_c RE-Ba-Cu-O (REBCO, RE stands for rare earth) bulk superconductors, which consist of a superconducting $REBa_2Cu_3O_y$ (RE123) matrix containing, RE_2BaCuO_5 (RE211) non-superconducting second phase inclusions, possess significantly high potential for applications. Additionally, the melt-textured high T_c superconductor enables flux pinning to be improved by introducing a fine dispersion of second phase precipitates, such as Y_2BaCuO_5 (Y211) and RE211, which act as strong pinning centers. Recent advances in melt-growth techniques enabled the fabrication of large single grain REBCO bulk superconductors with a high current-carrying capability through the enhancement of flux pinning and the reduction of weak links. The zone melt growth process is a good fabrication method to eliminate the weak links and obtain large grains with good alignment so as to increase the critical current density [1-7]. In the zone melt growth process, as there is no contact between the liquid and the support, liquid losses are avoided. So, this process is an efficient way for processing YBCO and REBCO bars with a high and sharp superconducting transition. In the melt-textured YBCO and REBCO systems, among various means to reduce the average 211 particle size, there are certain additions which minimize the coarsening of the 211 and help to refine the 211 size, with Ce and Pt-based additives being effective in this regard [8, 9]. Recently,

several research groups have reported that REBCO systems where two or three rare-earth elements are mixed can show very large values of critical current densities (J_c), when they are processed by an oxygen-controlled melt growth (OCMG) technique [10, 11]. However, the OCMG process has some drawbacks, including additional cost and equipment for commercialization. In this study, we report grain growth and superconducting properties of (YSN)-123 composite oxides with/without CeO_2 additive prepared by a zone melt growth process in air atmosphere where we have systematically investigated the microstructure of finely dispersed (YSN)211 nonsuperconducting inclusions in the (YSN)123 superconducting matrix.

Experimental Procedure

Preparation of Green Rods of the (YSN)-123 System

The directional melt growth process for fabricating (YSN)-123 composite oxides containing (YSN)211 second phase precipitates is as follows. High purity commercial powders of Y_2O_3 , Nd_2O_3 , Sm_2O_3 , $BaCO_3$, and CuO powders were weighed in appropriate amounts and mixed in an agate mortar according to the nominal composition of $(Y_{0.5}Sm_{0.25}Nd_{0.25})Ba_2Cu_3O_y$ [(YSN)-123]. Precursor powders were thoroughly ground and calcined at 880 °C for 30 h twice in air with intermediate grinding. It has been reported that CeO_2 is effective for increasing the viscosity of the Ba-Cu-O melts and can act as a growth inhibitor for RE211 particles [8, 12]. For these reasons, 1 wt% CeO_2 was added. All these powders [(YSN)-123+(YSN)211+ CeO_2] were mixed and milled with attrition for 6 h in ethanol using zirconia balls with a rotation speed 450 rpm. The (YSN)-123 powders milled with attrition were dried in

*Corresponding author:
Tel : +82-33-520-9322
Fax: +82-33-521-9407
E-mail: sjkim-jerome@hanmail.net

air, and then isostatically pressed at 200 MPa into a small cylindrical tubes (3 mm in inner diameter, 6 mm in outer diameter and 100 mm in length) using a rubber mould.

Melt-textured (YSN)-123 by the Zone Melt Process

The pre-heated (930 °C, 5 h) (YSN)-123 rod samples were processed in a vertical zone melting furnace, applying a thermal gradient (G) close to 200 Kcm^{-1} . Unidirectional solidification was obtained by moving the sample upward through a hot zone (T_m , $\sim 1100 \text{ °C}$) at a rate of about 3 mm/h in air. The zone melt growth apparatus used in this study is shown in Fig. 1. Details of the directionally melt growth conditions are summarized in Table 1. The post-heat treatment was performed at 450 °C in an oxygen gas atmosphere for 150 h in a separate tube furnace.

Characterization of Melt-textured (YSN)-123 Crystals

The directionally melt grown sample of (YSN)-123 was cleaved into smaller sections (2–3 mm long) for characterization. The microstructural observations were performed on well polished surfaces of the samples by means of scanning electron microscopy (SEM), optical microscopy, transmission electron microscopy (TEM), and high-resolution transmission electron microscopy (HR-TEM). The chemical compositions of the matrix and secondary phase were determined by energy dispersive x-ray spectrometer (EDS) analysis. Critical temperature (T_c) values were measured with a SQUID magnetometer (Quantum Design MPMS-7) in the zero field cooled (ZFC) mode in an applied magnetic field of 1 mT. Magnetization hysteresis (M-H) loops were

measured at 50 K in fields up to 5 T applied parallel to the c -axis.

Results and Discussion

Microstructure

In melt-processed high T_c bulk superconductors, microstructural control is the key parameter for successful industrial applications of these materials. In the REBCO and YBCO bulk systems, a large number of crystal defects are present in the RE123 matrix that can act as effective pinning centers [10]. Figure 2 shows a photograph of the directionally melt grown (YSN)-123 crystal by the zone melt growth process in air. Figure 3 shows a SEM micrograph of the fractured cross section transverse to the long axis of the directionally melt-textured (YSN)-123 crystal viewed in Fig. 2. In Fig. 3, we can see that the thin (YSN)-123 platelets (plate-type grains) are oriented parallel to the long axis and that the platelets extend across the entire cross section of the directionally melt-textured rod crystal.

Figure 4 shows that uniformly distributed (YSN)211 inclusions are trapped within the (YSN)123 matrix, and they have a platelet structure. As can be seen in Fig. 4, in the CeO_2 additive sample, the (YSN)211 inclusion size was remarkably reduced and the inclusions were finely dispersed within the (YSN)123 matrix. In the melt-processed REBCO bulk system, the RE211 inclusions tend to coarsen in the liquid (Ba-Cu-O) through an Ostwald ripening process. The CeO_2 additive is effective in suppressing the growth of RE211 inclusions. It is evident that the size of the (YSN)211 inclusions is depressed by the CeO_2 additive. This refinement of the size of (YSN)211 inclusions is observed for all samples.

In the melt growth processed REBCO bulk system, the pinning provided by the nonsuperconducting particles

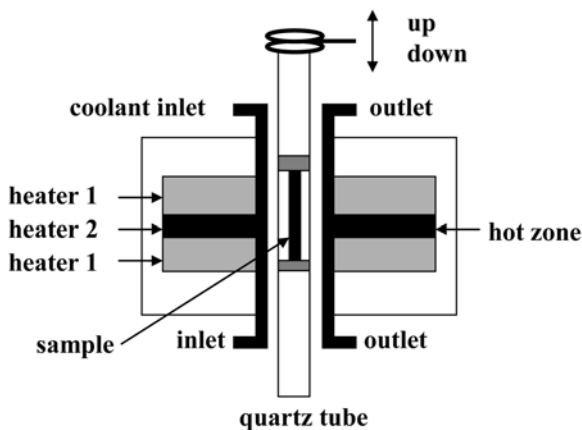


Fig. 1. Schematic illustration of the experimental apparatus for the zone melt growth method in air.

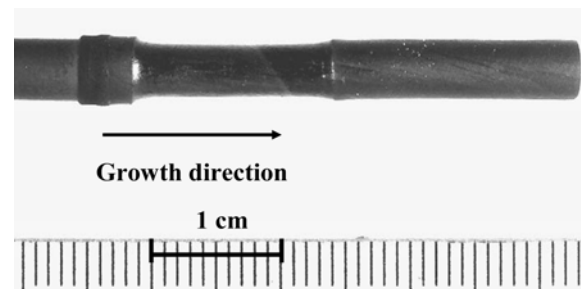


Fig. 2. Photograph of the directionally melt grown (YSN)-123 crystal.

Table 1. Melt growth conditions of the directionally melt-textured (YSN)-123 system in air

Sample	Melting temperature, T_m (°C)	Peritectic temperature, T_p (°C)	Growth rate, R (mm/h)	Superconducting transition temperature, T_c (K)
(YSN)-123	1100	1065	3	94
(YSN)-123+1 wt% CeO_2	1085	1060	3.5	94.5

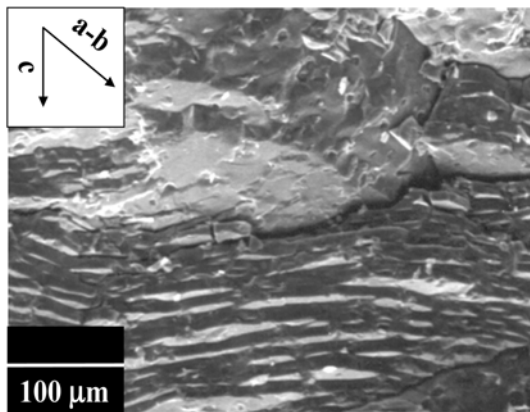


Fig. 3. SEM micrograph of the fractured cross section of the directionally melt-textured (YSN)-123 crystal viewed in Fig. 2.

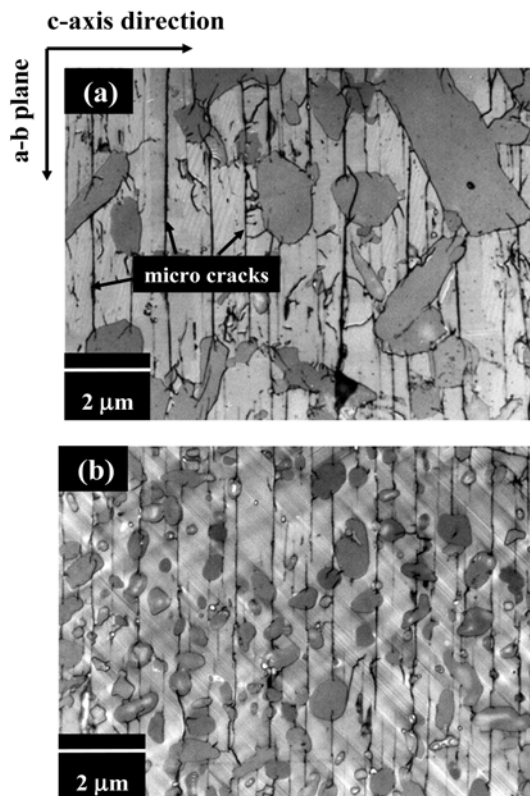


Fig. 4. Optical micrographs of the directionally melt-textured (a) (YSN)-123 and (b) (YSN)-123 crystal with 1 wt% CeO_2 additive. Note the finely dispersed (YSN)211 inclusions are trapped in the (YSN)123 matrix as platelet crystals.

of the RE211 phase is mainly effective at low magnetic fields and at high temperature above 77 K. In this case, the interfaces between the RE123 matrix and RE211 inclusions play an important role in the flux pinning, because the size of RE211 is much larger than the coherence length. In order to obtain more detailed information on the (YSN)211 inclusion size and distribution, we performed a transmission electron microscopy (TEM) study on the same sample. TEM was performed on the sample annealed at 450 °C for 100 h.

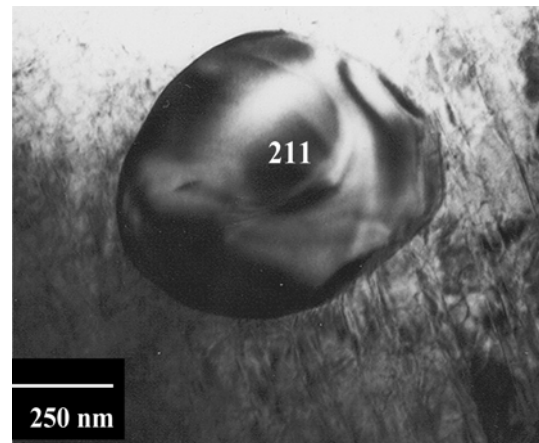


Fig. 5. TEM micrograph of the directionally melt-textured (YSN)-123 crystal with 1 wt% CeO_2 additive. The (YSN)211 inclusion, dense twin patterns and nano-sized defects are seen in the image.

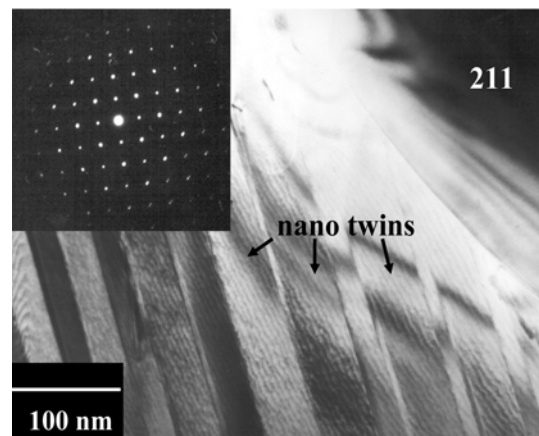


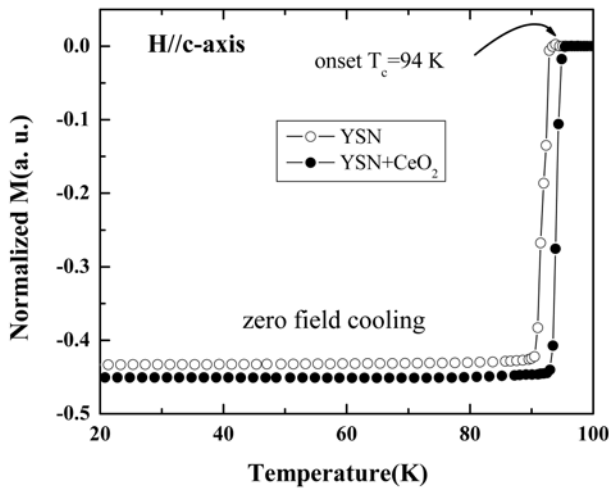
Fig. 6. High resolution TEM image and selected area electron diffraction (SAED) pattern of the directionally melt-textured (YSN)-123 crystal with 1 wt% CeO_2 additive. A SAED pattern shown in the inset indicates trapped phases are well crystallized.

Figure 5 shows a TEM bright field image around a (YSN)211 inclusion of the (YSN)123 matrix viewed from a [001] direction. As can be seen in Fig. 5, the existence of nano defects and a high density of dislocations in addition to the twin structure are observed. Also, twin and twin boundaries having about 50 nm spacing can be observed in Fig. 6.

To increase the superconducting properties, the total area of interface should be important; smaller Y211 and RE211 inclusions are more efficient in enhancing flux pinning [13, 14]. Figure 6 shows HR-TEM image and selected area electron diffraction (SAED) pattern around the (YSN)123 matrix and the (YSN)211 inclusion viewed from a [001] direction. As shown in Fig. 6, the (YSN)123 matrix is well crystallized. TEM-EDS analysis was performed on both the (YSN)123 matrix and (YSN)211 inclusions. As shown in Table 2, only homogeneous (YSN)123 and (YSN)211 are observed, and an impurity phase of RE is not found.

Table 2. TEM-EDS analysis on (YSN)123 matrix and (YSN)211 inclusion of as grown (YSN)-123 crystal shown in Fig. 6

Element(at%)	(YSN)123 matrix	(YSN)211 inclusion
Y	5.135	11.218
Sm	2.672	5.142
Nd	2.405	4.672
Ba	16.734	10.853
Cu	24.519	11.285

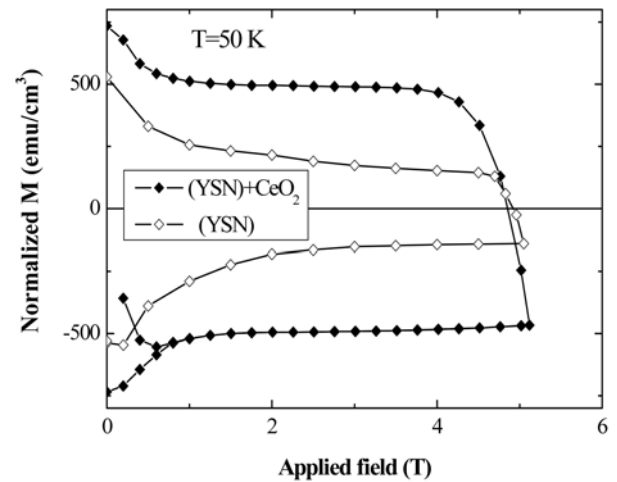
**Fig. 7.** Temperature dependence of the normalized magnetic susceptibility for the directionally melt-textured (YSN)-123 sample. The measurements were performed with a zero-field cooled (ZFC) warming procedure with an applied field of 1 mT and for H//c-axis direction.

Superconducting Properties

In order to find established that the sample contains a superconducting phase, the magnetic susceptibility of the directionally melt-textured (YSN)-123 sample was measured. A field of 1 mT was applied parallel to the c-axis from 20 to 100 K in a zero field cooled (ZFC) environment. As shown in Fig. 7, the (YSN)-123 sample with the CeO₂ additive shows a sharp superconducting transition at 94.5 K, indicating that the sample consists of a homogeneous superconducting phase. Figure 8 shows magnetization hysteresis (M-H) loops of the directionally melt-textured (YSN)-123 samples. Obviously, the (YSN)-123 sample with the CeO₂ additive exhibited higher T_c and M-H values than those for the other sample. It seems that the finely dispersed (YSN)211 inclusions within the (YSN)123 matrix is more effective in improving superconducting properties of the (YSN)-123 phase than the coarse (YSN)211 inclusions.

Conclusions

We have succeeded in the synthesis of a directionally melt-textured (YSN)-123 superconductor with CeO₂ additive by the zone melt growth process in an air atmosphere. The (YSN)211 nonsuperconducting inclu-

**Fig. 8.** Magnetization hysteresis (M-H) loops of the directionally melt-textured (YSN)-123 samples.

sions are uniformly dispersed within the (YSN)123 superconducting matrix. Both samples, (YSN)-123 and (YSN)-123 with the CeO₂ additive, showed an onset T_c ≥ 94 K and a sharp superconducting transition. The magnetization values of (YSN)-123 with the CeO₂ addition, were higher (M=500 emu/cm³ in 4 Tesla at 50 K) than those of (YSN)-123. These results indicate the finely dispersed (YSN)211 inclusions within the (YSN)123 matrix are more effective in improving superconducting properties of the (YSN)-123 phase than the coarse (YSN)211 inclusions.

References

1. P. McGinn, W. Chen, and M. Black, *Physica C* 161 (1989) 198-204.
2. D. Shi, H. Krishnan, J. Hong, and D. Miller, *J. Appl. Phys.* 68[1] (1990) 228-232.
3. S.J. Kim and H.G Kim, *Physica C* 338 (2000) 110-114.
4. F. Giovannelli, S. Marinelli, and I. Monot-Laffez, *Supercond. Sci. Technol.* 15 (2002) 533-538.
5. A. Ubaldini, F. Giovannelli, and I. Monot-Laffez, *Physica C* 33 (2002) 107-116.
6. S.J. Kim, *J. KIEEME.* 5[2] (2004) 81-85.
7. S.J. Kim, *J. KIEE.* 5-C[6] (2005) 251-256.
8. M.P. Delamare, M. Hervieu, J. Wang, J. Provot, I. Monot, K. Verbist, and G. Van Tendeloo, *Physica C* 262 (1996) 220-226.
9. R. Cloots, T. Koutzarova, J.P. Mathieu, and M. Ausloos, *Supercond. Sci. Technol.* 18 (2005) R9-23.
10. S. Awaji, N. Isono, K. Watanabe, M. Muralidhar, M. Murakami, N. Koshizuka, and K. Noto, *Supercond. Sci. Technol.* 17 (2004) S6-9.
11. M. Muralidhar, N. Sakai, M. Jirsa, and M. Murakami, *Physica C* 378 (2002) 646-650.
12. L. Shlyk, K. Nenkov, G. Krabbles, and G. Fuchs, *Physica C* 423 (2005) 22-28.
13. S. Sakai, N. Sakai, M. Murakami, and I. Hirabayashi, *Supercond. Sci. Technol.* 17 (2004) S30-S35.
14. M.R. Koblishka, M. Muralidhar, and M. Murakami, *Physica C* 337 (2000) 31-38.